Molecular Therapy
Nucleic Acids
Original Article

The Long Noncoding RNA D63785 Regulates Chemotherapy Sensitivity in Human Gastric Cancer by Targeting miR-422a

Zhixia Zhou,[1,4] Zhijuan Lin,[2,4] Yuqi He,[3] Xin Pang,[1] Yin Wang,[1] Murugavel Ponnusamy,[1] Xiang Ao,[1] Peipei Shan,[1] Muhammad Akram Tariq,[1] Peifeng Li,[1] and Jianxun Wang[1]

[1]Center for Tumor Molecular Biology, Institute for Translational Medicine, Qingdao University, Qingdao 266021, China; [2]Key Lab for Immunology in Universities of Shandong Province, School of Clinical Medicine, Weifang Medical University, Weifang 261053, China; [3]Department of Gastroenterology, Beijing Military General Hospital, Beijing 100700, China

Gastric cancer is one of the most prevalent tumor types in the world. Chemotherapy is the most common choice for cancer treatment. However, chemotherapy resistance and adverse side effects limit its clinical applications. Aberrant expression of long noncoding RNAs (lncRNAs) has been found in various stages of gastric cancer development and progression. In this study, we identified that an oncogenic lncRNA, long intergenic non-protein-coding RNA D63785 (lncR-D63785), is highly expressed in gastric cancer tissues and cells. Silencing of lncR-D63785 inhibited cell proliferation, cell migration and invasion in gastric cancer cell lines and reduced tumor volume and size in mice. We found that the expression of lncR-D63785 was inversely correlated with microRNA 422a (miR-422a) expression, which was involved in the downregulation of expression of myocyte enhancer factor-2D (MEF2D) and drug sensitivity. Knockdown of lncR-D63785 increased the expression of miR-422a and the sensitivity of gastric cancer cells to apoptosis induced by the anticancer drug doxorubicin (DOX). This indicates that lncR-D63785 acts as a competitive endogenous RNA (ceRNA) of miR-422a and promotes chemoresistance by blocking miR-422-dependent suppression of MEF2D. Together, our results suggest that the therapeutic suppression of lncR-D63785 alone or in combination with chemotherapeutic agents may be a promising strategy for treating gastric cancer.

INTRODUCTION

Gastric cancer is one of the most prevalent tumor types in the world, especially in East Asia.[1,2] It is the second most common cancer and the third leading cause of death from cancer in China. Like many other cancers, the molecular mechanisms of gastric cancer are very complex and poorly understood. Genetic mutations, epigenetic changes, and environmental factors play an important role in the development and progression of gastric cancer.[3,4] It is also known that gastric cancer is generally undetectable in the early stages because of the lack of novel molecular biomarkers for diagnosis.[5,6] In addition, current treatment options are still limited, and there are no precise and effective medical strategies.[7,8] Therefore, a high mortality rate is still observed in patients, and there is still a long way to go to achieve effective and less harmful treatments for gastric cancer.

Chemotherapy is the major clinical therapeutic regimen against various cancers in humans, including gastric cancer.[9–13] Commonly used chemotherapeutic agents, such as 5-fluorouracil (5-FU), cis-diaminedichloroplatinum (CDDP), and doxorubicin (DOX), often belong to the cytotoxic group of drugs that can directly kill tumor cells by inducing DNA double-strand break (DSB) damage and induce apoptosis.[10–13] However, the development of resistance to apoptosis induced by chemotherapeutic drugs during treatment drastically decreases the efficacy of chemotherapy and is a key mechanism of the therapeutic escape of cancer cells and a major obstacle to cancer therapy.[14–16] In addition, all clinical chemotherapeutic agents have severe adverse effects, such as cardiomyopathy, typhlitis, acute myelotoxicity, and other non-specific toxicities induced by high drug doses.[10–13] Thus, it is urgent to explore potential mechanisms involved in chemotherapy resistance, develop new drugs targeting drug-resistant tumors, and explore new compounds for combination therapy to enhance the therapeutic effects of anti-tumor drugs with minimal adverse effects.

Long ncRNAs (lncRNAs) are a class of non-protein-coding RNAs with a length of more than 200 nt, and they are generally considered to be mRNA-like transcripts.[17,18] lncRNAs have been involved in a variety of biological functions during evolutionary conservation, selection, and development, including chromatin imprinting, chromatin modification, and chromatin maintenance. In addition, lncRNAs are emerging as key players in the development and progression of various disease conditions, and they are aberrantly expressed in various types

Received 26 December 2017; accepted 11 May 2018;
https://doi.org/10.1016/j.omtn.2018.05.024.

[4]These authors contributed equally to this work.

Correspondence: Jianxun Wang, Center for Tumor Molecular Biology, Institute for Translational Medicine, Qingdao University, Qingdao 266012, China.
E-mail: wangjx@qdu.edu.cn
Correspondence: Peifeng Li, Center for Tumor Molecular Biology, Institute for Translational Medicine, Qingdao University, Qingdao 266012, China.
E-mail: peifeng@ioz.ac.cn

of human diseases, including cancer.[3,4,19] In gastric cancer, many lncRNAs have been reported to be closely associated with the occurrence, development, invasion, and metastasis of tumors as well as drug resistance. For example, H19,[20] HOTAIR,[21] HOTTIP,[22] and linc00673,[23] which are upregulated in gastric cancer, can accelerate gastric cancer tumorigenesis by inhibiting target genes in *cis* or in *trans*. In contrast, GAS5[24,25] and MEG3[26,27] are downregulated in gastric cancer, and they function as tumor suppressor genes to inhibit the development and progression of gastric cancer. In addition, some lncRNAs, such as MRUL[28], HULC[29] and UCA1,[30] have oncogenic roles in gastric cancer by modulating resistance to chemotherapeutic agents. In this background, it might be possible to functionally manipulate lncRNAs as diagnostic or prognostic biomarkers, novel therapeutic targets, and/or adjuvant compounds with chemotherapy in gastric cancer treatment.

The gene-regulatory functions of lncRNAs during development, physiology, and pathology are diverse and complex. They act as signals, decoys, guides, and scaffolds, among others, at transcriptional, post-transcriptional, and epigenetic levels.[17–19] Recently, a new regulatory mechanism of gene expression by lncRNAs was identified. In that case, lncRNAs function as competing endogenous RNAs (ceRNAs) to sponge microRNAs (miRNAs), antagonizing miRNAs and modulating the depression of their target mRNAs.[31,32] In previous reports, MALAT-1,[33] lncRNA-ATB,[34,35] and H19[20,36,37] were identified as ceRNAs that protect their target mRNAs from miRNA-mediated degradation in many cancers. Hence, the complex regulatory network of lncRNA-miRNA crosstalk implies the possibility of cancer diagnosis and therapy.

In a primary screening of global lncRNA expression profiles in gastric cancer using a microarray, we found that the lncRNA D63785 (lncR-D63785; Ensembl: uc002h1t.l) is highly expressed in gastric cancer tissues and that it is located on the chromosome 17: 34.610.748-34.611.354 antisense strand with a length of 185 nt. However, its role in cancer was unclear. In this study, we further analyzed the expression of lncR-D63785 in gastric cancer patients and cell lines. Our results showed that knockdown of lncR-D63785 in a gastric cancer cell line inhibited cell proliferation, migration, and invasion. Moreover, we revealed that silencing of lncR-D63785 enhanced chemotherapeutic sensitivity in gastric cancer cells through the miR-422a-myocyte enhancer factor-2D (MEF2D) axis *in vitro* and *in vivo*, which highlights the possible development of new treatment strategies for gastric cancer.

RESULTS

lncR-D63785 Is Upregulated in Human Gastric Cancer Tissues and Cell Lines

Using a microarray, we obtained the differential expression profiles of lncRNAs between gastric cancer samples and paired non-cancerous specimens. We found that lncR-D63785 was one of the most upregulated lncRNAs in gastric cancer and that it is a 185-nt antisense lncRNA transcribed from a gene located on chromosome 17 (Figure 1A). The expression level of lncR-D63785 was further confirmed by real-time qPCR in gastric cancer tissues and pair-matched adjacent normal gastric tissues from 21 gastric carcinoma patients. As shown in Figures 1B and 1C, the expression of lncR-D63785 was significantly elevated in tumor tissues of 61.9% (13 of 21) of gastric cancer patients compared with their matched adjacent normal tissues, with an average difference of approximately 5-fold ($p < 0.05$). Moreover, we found that a higher lncR-D63785 expression level was significantly correlated with decreased overall survival during the first 3 years after gastric cancer diagnosis (Figure 1D). We also performed real-time qPCR analysis to examine the expression levels of lncR-D63785 in gastric cancer cell lines (SGC7901, MGC803, BGC823, and NCI-N87) and compared it with a normal gastric epithelium cell line (GES-1). The results showed that lncR-D63785 was markedly increased in BGC823 and NCI-N87 cells (Figure 1E). These results indicate that lncR-D63785 might play a pivotal role in the pathogenesis of gastric carcinoma.

lncR-D63785 Acts as an Oncogene by Promoting Cell Proliferation, Migration, and Invasion of Gastric Cancer Cells

lncR-D63785 was expressed at high levels in most of the gastric cancer tissues and cell lines. Next we explored the function of this lncRNA in tumorigenesis and development of gastric cancer. For this experiment, we silenced the expression of endogenous lncR-D63785 using a more specific small interfering RNA (siRNA), as shown in Figure 1F, and cells were grown for up to 96 hr. Based on the methylthiazolyldiphenyl-tetrazolium bromide (MTT) assay, a significant reduction in cell viability was observed in cells transfected with siRNA-D63785 compared with those transfected with control siRNA (Figure 1G). Cell viability was also tested using an 5-ethynyl-2'-deoxyuridine (EdU) incorporation assay, and similar results were obtained (Figure 1H). As another important indicator of tumor cell activity, we examined cell migration and invasion by transwell assay after knockdown of lncR-D63785. We observed that the migratory and invasive abilities of BGC823 cells were remarkably reduced upon silencing of lncR-D63785 compared with untreated control cells (Figure 1I). Similarly, the effects of lncR-D63785 silencing on cell proliferation (Figure S1A) and migration and invasion (Figure S1B) were also obtained for NCI-N87 cells. We enhanced lncR-D63785 expression by transfecting BGC823 cells with an lncR-D63785 expression vector (pCR3.1-D63785) (Figure S2A). We found that lncR-D63785 overexpression did not influence cell proliferation (Figure S2B) or migration and invasion (Figure S2C). However, when lncR-D63785 was overexpressed in the low-lncR-D63785-expressing cell line MGC803 (Figure S2D), cell proliferation (Figure S2E) and migration and invasion (Figure S2F) were significantly enhanced, which indicated that BGC823 cells were suitable for loss-of-function assays and MGC-803 cells were suitable for gain-of-function assays. These results suggest that the increased expression of lncR-D63785 in gastric carcinoma cells is associated with the development and progression of gastric cancer.

Silencing of lncR-D63785 Enhanced the Sensitivity of Gastric Cancer Cells to Chemotherapy by Inducing Apoptosis

Next we examined whether lncR-D63785 has any influence on gastric cancer cell apoptosis by knockdown of lncR-D63785 in BGC823 cells. As shown in Figure 2A, although the number of apoptotic cells was

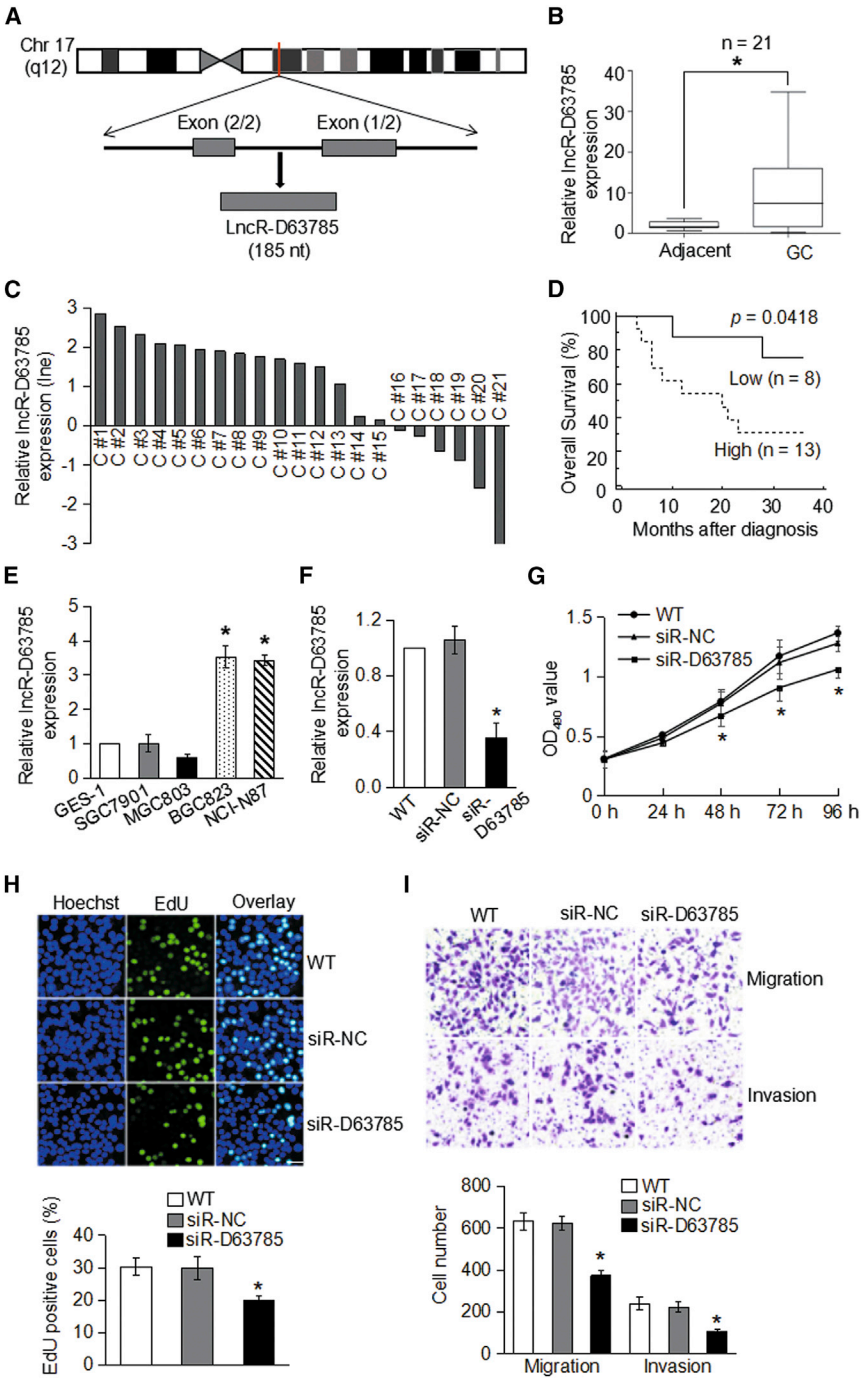

Figure 1. lncR-D63785 Acts as an Oncogene in Gastric Cancer

(A) Schematic representation of the genomic location of lncR-D63785. (B) The relative expression of lncR-D63785 in gastric cancer (GC) tissues was examined by real-time qPCR, normalized to GAPDH expression, and compared with the paired adjacent normal tissues with one normal tissue expression level as 1 (n = 21); *p < 0.05 versus the adjacent group. (C) lncR-D63785 expression (lne ratio) was classified into two groups, the high expression group (up) and the low expression group (down), compared with their corresponding adjacent normal tissues. (D) Kaplan-Meier analysis of the correlation between lncR-D63785 expression levels and 3-year overall survival; p = 0.0418. (E) The mRNA levels of lncR-D63785 in cancer cells lines (SGC7901, MGC803, BGC823, and NCI-N87) were compared with corresponding normal gastric epithelial cells (GES-1); *p < 0.05 versus the GES-1 group. (F) The relative expression level of lncR-D63785 in BGC823 cells transfected with siR-NC or siR-D63785 was tested by real-time qPCR. (G) 24 hr, 48 hr, 72 hr, and 96 hr after transfection with siR-D63785, a MTT assay was performed to determine the proliferation of BGC823 cells, which was shown as the absorbance at optical density 490 (OD_{490}). (H) 48 hr after transfection, cell proliferation was tested using an EdU incorporation assay. Up: representative figures. Scale bars, 50 μm. Down: percentages of EdU-positive cells. (I) Cell migration and invasion were evaluated after 48 hr of incubation by transwell assay. Up: representative figures. Scale bars, 50 μm. Down: cell counts of stained cells. *p < 0.05 compared with the siR-NC treatment group. Data are expressed as the mean ± SD from at least three separate experiments.

increased with increasing the concentration of siRNA-D63785, there was no significant difference compared with the control group. Several studies[10–13] have shown that tumor cell resistance to apoptosis is associated with drug resistance. In this context, our results showed that the knockdown of endogenous lncR-D63785 could not influence cell apoptosis. Therefore, we evaluated whether lncR-D63785 participates in the regulation of DOX-induced tumor cell apoptosis and whether inhibition of endogenous lncR-D63785 could increase the sensitivity of tumor cells to DOX. First we examined the effect of DOX on the expression of lncR-D63785. Interestingly, we observed a time-dependent decrease in the level of lncR-D63785 following treatment with DOX in BGC823 cells (Figure 2B). To our surprise, we found that, when DOX was removed, lncR-D63785 expression recovered quickly (Figure S3). During further study, we found that pre-incubation with siR-D63785 led to increased susceptibility of BGC823 cells to DOX-induced cytotoxicity (Figure 2C). Interestingly, the higher dose (2 μM) of DOX-induced cell apoptosis was significantly decreased in cells overexpressing lncR-D63785, but lncR-D63785 alone did not influence cell apoptosis (Figure 2D). The effects of lncR-D63785 on DOX-induced cell apoptosis were also investigated in NCI-N87 cells, and similar results were obtained (Figures S4A and S4B). In addition, we also found that knockdown of lncR-D63785 did not influence apoptosis of MGC803 cells but had a stronger ability to enhance the chemotherapy sensitivity of MGC803 cells

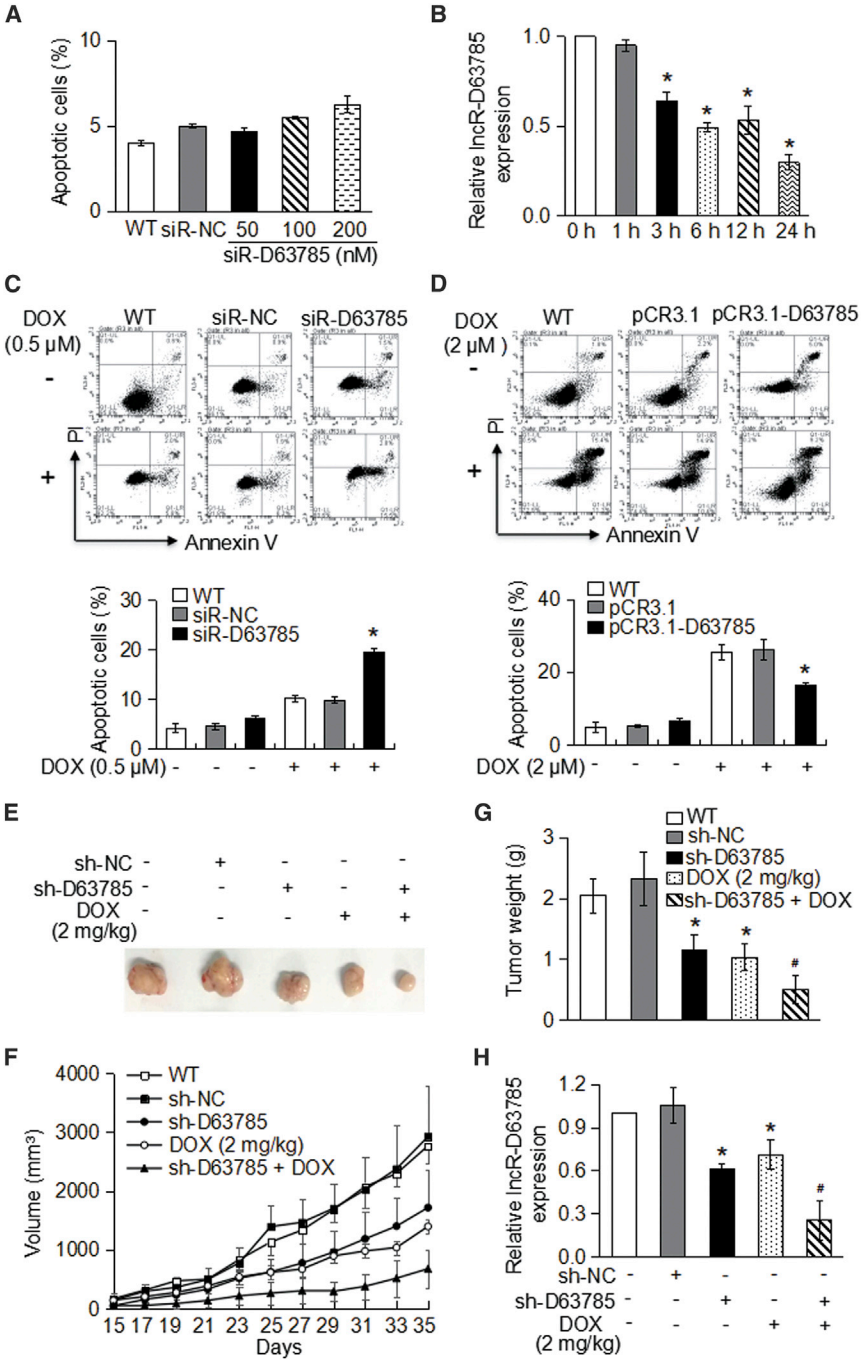

Figure 2. Effects of lncR-D63785 on DOX-Mediated Toxicity *In Vitro* and *In Vivo*

(A) BGC823 cells were transfected with siR-NC (100 nM) or siR-D63785 at the indicated concentrations (50 nM, 100 nM, and 200 nM) for 48 hr, and then the cells were stained with Annexin V and PI and subjected to fluorescence-activated cell sorting by flow cytometry; *p < 0.05 compared with the siR-NC treatment group. (B) BGC823 cells were treated with DOX at a concentration of 2 μM for the indicated times (0 hr, 1 hr, 3 hr, 6 hr, 12 hr, and 24 hr), and the expression of lncR-D63785 was tested by real-time qPCR; *p < 0.05 compared with the 0 hr treatment group. (C) BGC823 cells were transfected with siR-NC (100 nM) or siR-D63785 (100 nM) for 24 hr, and then cells were incubated with or without 0.5 μM DOX for another 24 hr. Apoptosis was detected by flow cytometry (up), and the percentages of apoptotic cells are presented as a bar chart (down); *p < 0.05 compared with the DOX plus siR-NC treatment group. (D) In addition, apoptosis in BGC823 cells treated with pCR3.1-D63785 or pCR3.1 as well as 2 μM DOX was also analyzed by flow cytometry; *p < 0.05 compared with the pCR3.1 treatment group. Data are expressed as the mean ± SD from at least three separate experiments. (E–H) BALB/c nude mice were injected subcutaneously with 1.5×10^6 BGC823 cells transfected with sh-D63785 or sh-NC. On day 15, when the tumors had reached 250–300 mm^3, the mice were administered DOX (2 mg/kg) by intraperitoneal injection every other day, whereas the control mice were injected with a corresponding volume of PBS. Then the mice were sacrificed on day 35. The tumors in each mouse were separated (E), and the tumor growth curves (F) and weights (G) were calculated. The expression of lncR-D63785 in tissues of resected tumors was also analyzed by real-time qPCR (H). *p < 0.05 compared with the sh-NC group, #p < 0.05 compared with the DOX treatment group.

to DOX than of BGC823 cells or NCI-N87 cells (Figure S4C). These results indicate that lnRNA-D63785 could be related to DOX resistance in human gastric cancer.

lncR-D63785 Is Involved in Gastric Tumor Growth and Chemotherapy Effectiveness *In Vivo*

Next we assessed whether lnRNA-D63785 could participate in tumor drug resistance in an animal model. The anti-tumor effects of lncR-D63785 knockdown alone or together with DOX were tested in nude mice bearing human BGC823 gastric carcinoma xenografts. First, lncR-D63785 short hairpin RNA (shRNA) lentiviral vectors were constructed, packaged to produce lentiviruses, and transduced into human BGC823 cells to obtain stable lncR-D63785 knockdown cells. We confirmed that the expression of lncR-D63785 was knocked down in lentivirus-infected BGC823 cells by fluorescence microscope and real-time PCR (data not shown). sh-D63785 lentivirus-infected BGC823 cells (1.5×10^6) or sh-negative control (NC) lentivirus-infected cells were injected subcutaneously into the right flanks of mice. On day 15 after tumor injection, when the tumors had reached 250–300 mm^3, the mice were administered DOX (2 mg/kg) by intraperitoneal injection every other day, whereas the control mice received a corresponding volume of PBS. When the treated mice were sacrificed on day 35, we found that both the size (Figure 2E) and volume (Figure 2F) of the tumor nodules were significantly

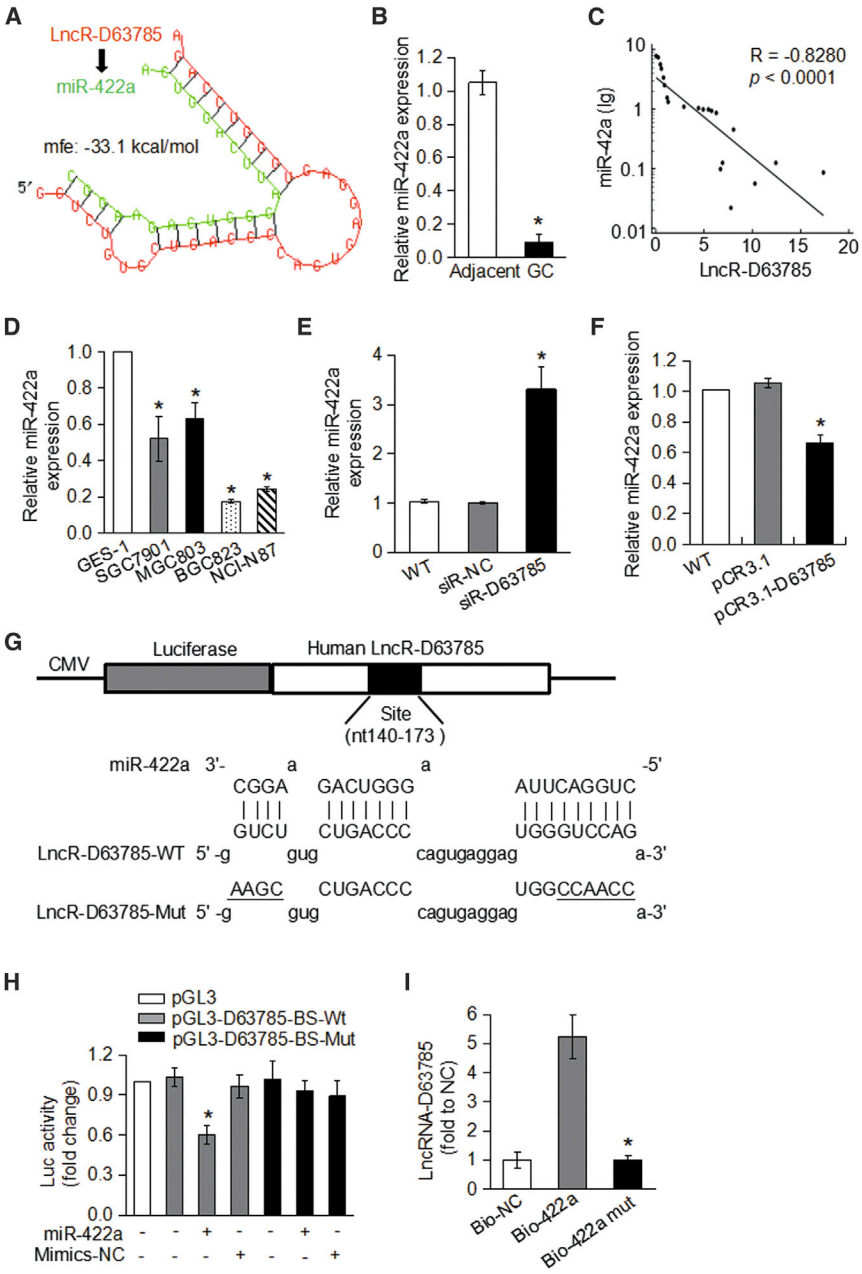

Figure 3. lncR-D63785 Interacts with miR-422a and Regulates Its Expression

(A) The 20 putative miR-422a-binding sites in the lncR-D63785 sequence. (B) The miR-422a level was determined by real-time qPCR in 21 surgical specimens of human GC tissues and normalized to those in the adjacent normal tissues; *p < 0.05 versus the adjacent group. (C) Spearman analysis was used to analyze the association between lncR-D63785 and miR-422a expression; R = −0.8280, p < 0.001. (D) miR-422a expression in GC cell lines (SGC7901, MGC803, BGC823, and NCI-N87) was compared with a normal human gastric epithelial cell line (GES-1) by real-time qPCR; *p < 0.05 versus the GES-1 group. (E and F) Expression of miR-422a in siR-D63785- or siR-NC-transfected BGC823 cell lines (E) and in pCR3.1-D63785- or pCR3.1-transfected BGC823 cell lines (F); *p < 0.05 versus the siR-NC or pCR3.1 treatment group. (G) Schematic representation of the constructs of pGL3-D63785-BS-WT and pGL3-D63785-BS-Mut containing the miR-422a binding site. The wild-type lncR-D63785 containing the binding site of miR-422a (D63785-BS-WT) (up) or its mutant (D63785-BS-Mut) (down) were cloned into pGL3 as indicated. The mutant sites are underlined. HEK293T cells were co-transfected with miR-422a or NC and luciferase constructs containing the wild-type lncR-D63785 binding site (pGL3-D63785-BS-WT) or a mutated lncR-D63785 binding site (pGL3-D63785-BS-Mut). (H) Luciferase activity was analyzed to determine the binding of miR-422a to lncR-D63785; *p < 0.05 versus pGL3-D63785-BS-WT alone. (I) BGC823 cells were transfected with biotinylated miR-422a (Bio-422a) or its mutant form (Bio-422a-Mut), and then a biotin-based pull-down assay was performed to detect lncR-D63785 expression and normalized to a biotinylated mimic control (Bio-NC) by real-time qPCR; *p < 0.05 compared with Bio-NC. Data are expressed as the mean ± SD from at least three separate experiments.

reduced in sh-D63785-treated mice, particularly the nodules in sh-D63785 plus DOX-treated mice. As shown in Figure 2G, the tumor weight in the sh-NC group increased to 2.32 ± 0.44 g, whereas it was only 1.15 ± 0.25 g in the sh-D63785 group, 1.03 ± 0.22 g in the DOX group, and 0.5 ± 0.23 g in the sh-D63785 plus DOX group. We also observed a decrease in the expression of lncR-D63785 in sh-D63785 or DOX tumor tissues, particularly sh-D63785 plus DOX tumor tissues (Figure 2H). These results indicate that lncR-D63785 contributes to DOX-induced chemosensitivity of gastric tumors *in vivo*.

miR-422a Is Downregulated by lncR-D63785 in Gastric Cancer

To explore the mechanism associated with chemosensitivity upon lncR-D63785 knockdown, we assessed whether lncR-D63785 can interact with some miRNAs because it has been reported that lncRNAs may act as an endogenous sponge RNA to interact with miRNAs and influence their expression.[31,32] Thus, we compared the sequence of lncR-D63785 with miRNAs using the bioinformatics program RNAhybrid and found some potential miRNAs, including miR-422a, containing target sites of lncRNA-D6378 (Figure 3A). Consequently, we examined the expression of miR-422a in the 21 surgical specimens of human gastric cancer cancer tissues and the adjacent normal tissues as tested above, and we found that there was a significant decrease in the expression of miR-422a in gastric cancer tissues (Figure 3B). The lower lncR-D63785 expression level was significantly correlated with increased overall survival (Figure S5A). We also found a statistically significant

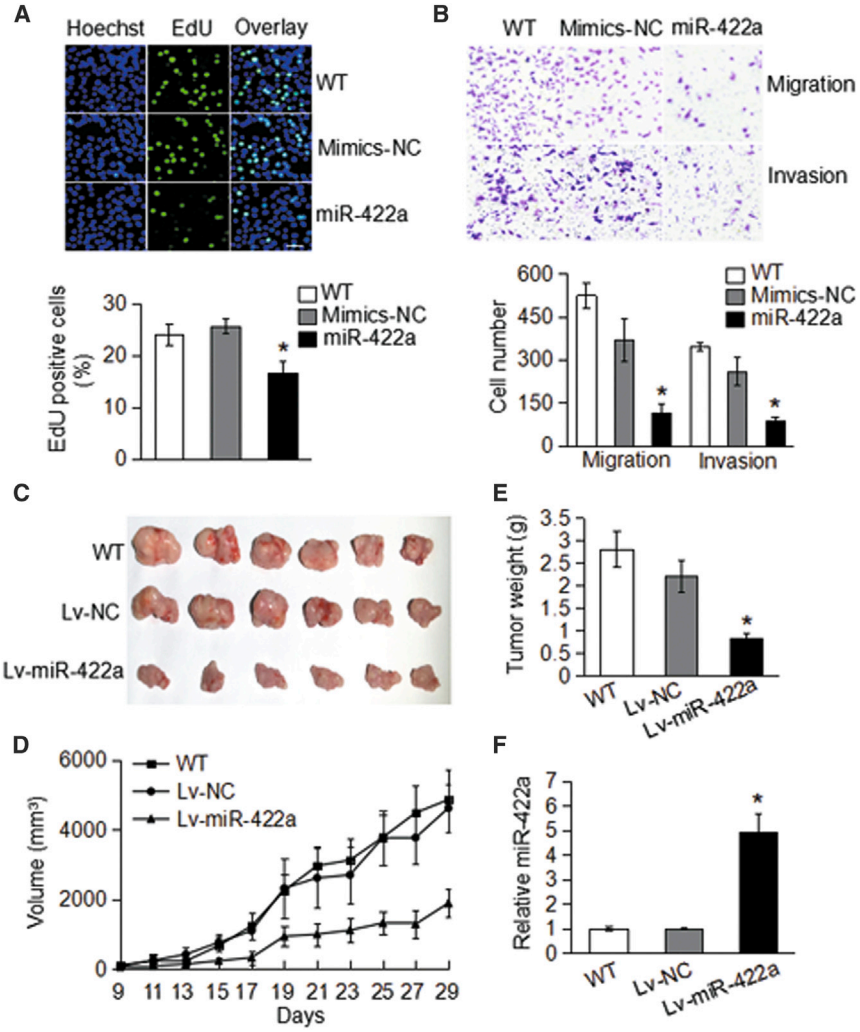

Figure 4. The Antitumor Effects of miR-422a *In Vitro* and *In Vivo*

(A) BGC823 cells were transfected with miR-422a or NC for 48 hr, and cell proliferation was tested using the EdU incorporation assay. Up: representative figures. Scale bars, 50 μM. Down: percentages of EdU-positive cells. *$p < 0.05$ compared with NC. (B) Cell migration and invasion were evaluated by transwell assay. Up: representative figures. Scale bars, 50 μM. Down: cell counts of stained cells. Data are expressed as the mean ± SD from at least three separate experiments; *$p < 0.05$ compared with NC. (C–F) BALB/c nude mice were injected subcutaneously with 2×10^6 BGC823 cells transfected with Lv-miR-422a or Lv-NC. The treated mice were sacrificed on day 30. The tumors in each mouse were separated (C); tumor growth curves (D) and weight (E) were calculated. The expression of miR-422a in tissues of resected tumors was also analyzed by real-time qPCR (F). *$p < 0.05$ compared with the Lv-NC group.

inverse correlation between the expression levels of miR-422a and lncRNA-D6378 in gastric cancer tissues (Figure 3C). In addition, miR-422a expression was downregulated in all detected gastric cancer cell lines, particularly BGC823 and NCI-N87 cells, compared with normal GES-1 cells, as assessed by real-time qPCR using Roche SYBR Green Supermix (Figure 3D) and the QIAGEN miScript SYBR Green PCR Kit and miScript Primer Assay (Figure S5B).

Next we examined whether miR-422a expression is regulated by lncR-D63785, and we found that the level of miR-422a was elevated in BGC823 cells following knockdown of endogenous lncR-D63785 (Figure 3E). In contrast, forced expression of lncR-D63785 led to a dramatic reduction in the level of miR-422a in BGC823 cells (Figure 3F), particularly in MGC803 cells (Figure S6A). Next we verified whether lncR-D63785 directly targets miR-422a by using the lncR-D63785 fragment containing the miR-422a binding site downstream of the luciferase reporter gene (D63785-BS-wild-type [WT]) (Figure 3G). We also generated a mutated luciferase construct (D63785-BS-Mut) in which mutations were introduced into the miR-422a binding site (Figure 3G). We found that miR-422a induced a decrease in luciferase activity, whereas introduction of the mutation substantially reduced the inhibitory effect of miR-422a (Figure 3H). In addition, biotin-avidin pull-down assay results showed that lncR-D63785 was pulled down by biotinylated miR-422a but not by mutant miR-422a (Figure 3I). These data suggest that lncR-D63785 directly binds to miR-422a and regulates its level in gastric cancer tissue.

miR-422a Reduces the Tumorigenesis of Gastric Cancer Cells

The expression of miR-422a is decreased in several types of tumors, including non-small-cell lung cancer (NSCLC), glioblastoma, and osteosarcoma, in which it acts as a tumor suppressor.[38–43] To test the potential tumor-suppressing role of miR-422a in gastric cancer, we used inhibitors to knock down endogenous miR-422a (Figure S6B) and mimics to increase miR-422a level (Figure S6C). We found that forced expression of miR-422a inhibited cell proliferation (Figure 4A) and migration and invasion (Figure 4B) of the BGC823 cell line. In addition, we tested the anti-tumor effects of miR-422a *in vivo* using nude mice bearing human BGC823 gastric carcinoma xenografts. BGC823 cells were infected with miR-422a lentiviruses or NC lentiviruses injected subcutaneously into the right flanks of mice. The tumor volume was measured every other day from day 9, when the tumors had reached 250–300 mm^3 in control mice. The treated mice were then sacrificed on day 30. The size (Figure 4C), volume (Figure 4D), and weight (Figure 4E) of the tumor nodules were significantly reduced in mice bearing miR-422a lentivirus-infected cells. We also observed an increase in the expression of miR-422a in lentiviral vector (Lv)-miR-422a tumor tissues (Figure 4F). These results show that miR-422a acts a tumor suppressor gene.

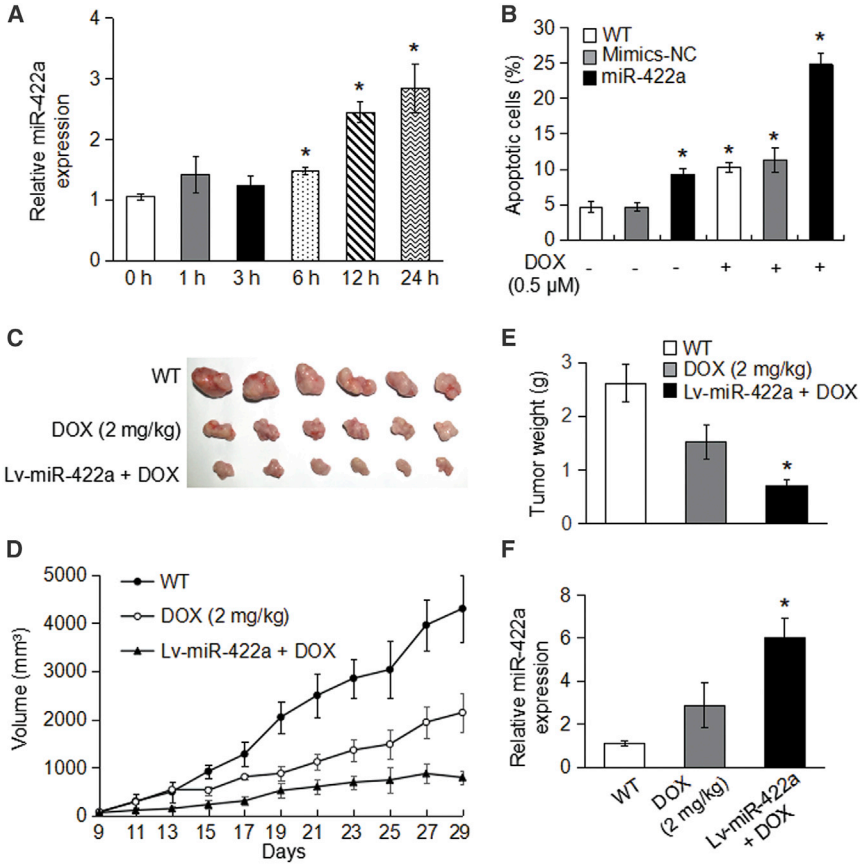

Figure 5. Effects of miR-422a on DOX-Induced Apoptosis in BGC823 Cell Lines

(A) The expression level of miR-422a was analyzed by real-time qPCR in BGC823 cells exposed to 2 μM DOX; *$p < 0.05$ versus 0 hr. BGC823 cells were transfected with miR-422a or NC for 24 h and then incubated with or without 0.5 μM DOX for another 24 hr. (B) The cells were stained with Annexin V and PI, and the percentages of apoptotic cells were analyzed by flow cytometry; *$p < 0.05$ compared with the NC alone group. Data are expressed as the mean ± SD from at least three separate experiments. (C–F) BALB/c nude mice were injected subcutaneously with 2×10^6 BGC823 cells transfected with Lv-miR-422a or Lv-NC. Beginning on day 9, when the tumors had reached 250–300 mm^3, the experimental mice were administered DOX (2 mg/kg) by intraperitoneal injection every other day, whereas the control mice were injected with a corresponding volume of PBS. All mice were sacrificed on day 30. (C–E) The tumors in each mouse were separated (C); tumor growth curves (D) and weight (E) were calculated. (F) The expression levels of miR-422a in tissues of resected tumors were analyzed by real-time qPCR; *$p < 0.05$ compared with the DOX treatment group.

miR-422a Enhances the Sensitivity of Gastric Cancer to Chemotherapy

Because we observed that the increased expression of lncR-D63785 leads to resistance to DOX-induced apoptosis in gastric cancer cells and that miR-422a expression is suppressed in those cells, we examined whether miR-422a has a functional role in the DOX-related chemosensitivity of gastric cancer. BGC823 cells were exposed to 2 μM DOX for different times (0–24 hr), and the level of miR-422a was examined by real-time qPCR. The results showed that the miR-422a level was markedly elevated 6 hr after DOX stimulation (Figure 5A) and steadily increased several fold after 24 hr, a time point when gastric cancer cell death was significantly increased. Transfection with the miR-422a mimic alone had a slight effect on cell apoptosis, whereas forced expression of miR-422a sensitized BGC823 cells to apoptosis induced by 0.5 μM DOX, as indicated by a remarkable increase in apoptotic cells (Figure 5B).

To confirm the anti-tumor effect of miR-422a and its enhancement in DOX-induced apoptosis, nude mice were grafted with BGC823 cells (2×10^6) infected with Lv-miR-422a or Lv-NC and were given an intraperitoneal injection of DOX (2 mg/kg) every other day, whereas the control mice were injected with a corresponding volume of PBS. The Lv-miR-422a plus DOX-treated mice had reduced size (Figure 5C), volume (Figure 5D) and weight (Figure 5E) of tumor nodules compared with the DOX-treated control mice. As expected, the level of miR-422a in Lv-miR-422a plus DOX-treated mice was higher than that in DOX-treated mice (Figure 5F). These results indicate that miR-422a has an enhancer activity in DOX-mediated chemosensitivity and cell death.

MEF2D Is a Target of miR-422a

We further searched for the target genes of miR-422a using a bioinformatics program, TargetScan, and found that *MEF2D* mRNA contained a potential target site of miR-422a in its 3′ UTR (Figure 6A). The protein level of MEF2D in human gastric cancer cancer tissues was much higher than that in adjacent normal tissues (Figure 6B). Further, we found that a higher MEF2D expression level was significantly correlated with decreased overall survival (Figure 6C). A statistically significant inverse correlation between the expression levels of MEF2D and miR-422a was also found in gastric cancer tissues (Figure 6D). Additionally, MEF2D expression was significantly increased in the majority of detected gastric cancer cell lines (3 of 4) compared with GES-1 (Figure 6E). It is well known that MEF2D is involved in the progression of tumor growth in various cancers, including gastric cancer.[44–48] To investigate the effects of MEF2D on the growth of gastric cancer cells, siRNA (siR-*MEF2D*) was used to knock down the MEF2D level (Figure S7A). The pKC-*EF1α*-*MEF2D* plasmid was used to overexpress MEF2D (Figure S7B). Knockdown of MEF2D expression markedly inhibited BGC823 cell proliferation (Figures S7C and S7D) and migration and invasion (Figures S7E

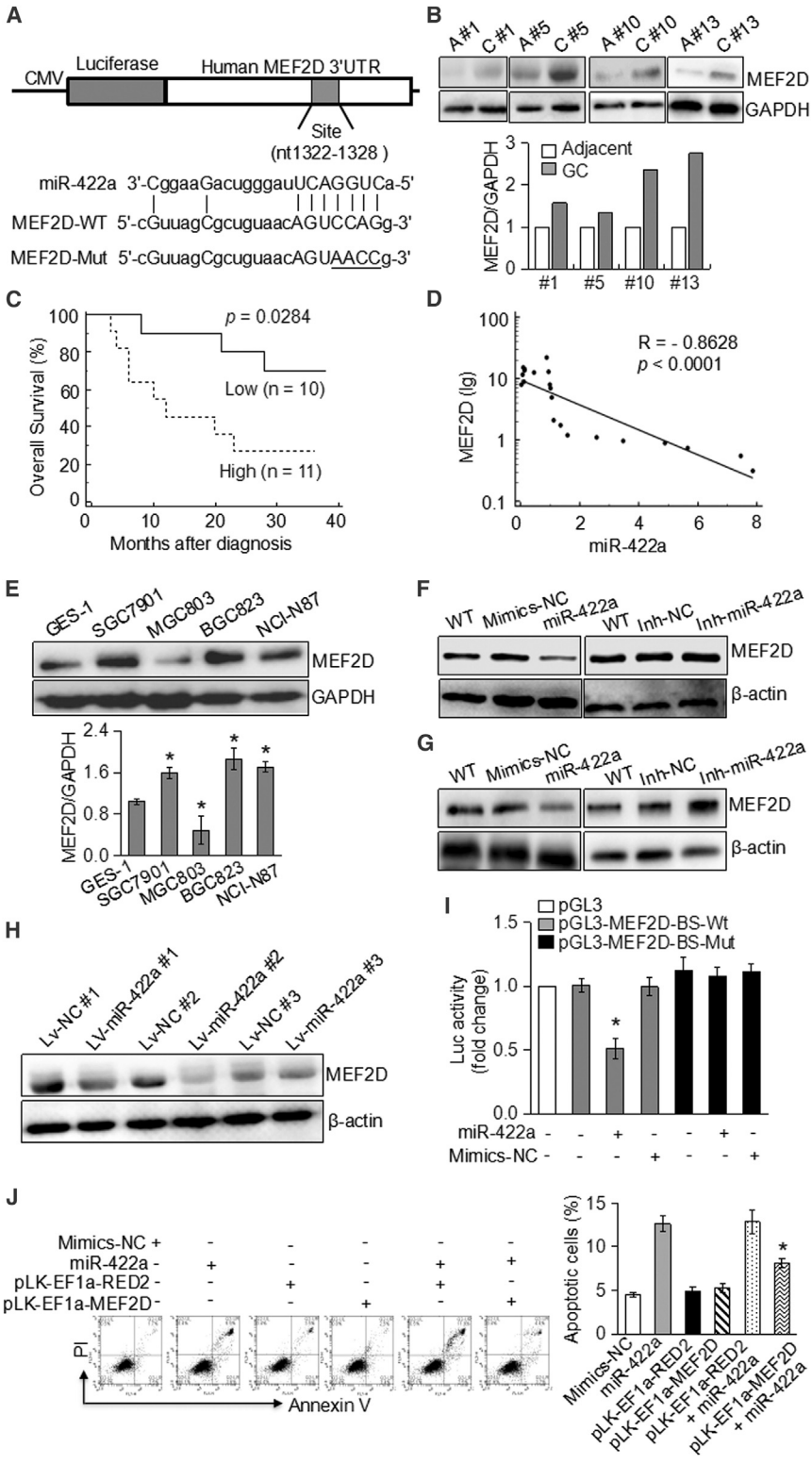

Figure 6. miR-422a Interacts with MEF2D and Regulates MEF2D Expression

(A) Putative miR-422a binding sites in the 3′-UTR of *MEF2D*. The wild-type *MEF2D* CDS containing the binding site of miR-422a (*MEF2D*-BS-WT) (up) or its mutant (*MEF2D*-BS-Mut) (down) were cloned into pGL3 as indicated. The mutant sites are underlined. (B) The MEF2D levels were determined in human GC tissues and adjacent normal tissues by western blotting (up), and the density of blots was quantified by MBF ImageJ software (down). (C) Kaplan-Meier analysis of the correlation between MEF2D expression levels and 3-year overall survival; p = 0.0284. (D) Spearman analysis was used to analyze the association between miR-422a and MEF2D expression; R = −0.8628, p < 0.001. (E) The MEF2D levels were determined in human GC cell lines by western blotting (up), and the quantification of band intensity relative to β-actin intensity of (A) was quantified by MBF ImageJ software (down); *p < 0.05 versus the GES-1 group. (F and G) BGC823 cells (F) and BGC823 cells (G) were transfected with mimics-miR-422a (left) and inhibitor-miR-422a (right) or their negative control mimics-NC (left) and inhibitor-NC (right) for 24 hr, and the MEF2D levels were determined by western blotting. (H) In xenograft tumor tissues in BALB/c nude mice, the expression level of MEF2D was analyzed by western blotting. HEK293 cells were transfected with miR-422a or NC and then transfected with the luciferase constructs of the wild-type MEF2D binding site (pGL3-*MEF2D*-BS-WT) or a mutated *MEF2D* binding site (pGL3-*MEF2D*-BS-Mut). (I) Subsequently, luciferase activity was analyzed to determine the binding of miR-422a to MEF2D; *p < 0.05 versus pGL3-*MEF2D*-BS-WT alone. (J) Apoptosis of BGC823 cells transfected with mimics-422a and pKC-*EF1α-MEF2D* or pKC-*EF1α-RED2* was detected by flow cytometry (left), and the percentages of apoptotic cells are presented as a bar chart (right); *p < 0.05 versus mimics-422a plus pKC-*EF1α-RED2*. Data are expressed as the mean ± SD from at least three separate experiments.

and S7F). However, forced expression of MEF2D had no obvious effect on cell viability (data not shown).

Next we investigated whether MEF2D expression is regulated by miR-422a. Forced expression of miR-422a led to a reduction in the level of MEF2D both in BGC823 cells (Figure 6F, left) and MGC803 cells (Figure 6G, left). Although knockdown of miR-422a cannot influence the expression level of MEF2D in BGC823 cells (Figure 6F, right), it can significantly increase MEF2D expression in the low-lncR-D63785-expressing cell line MGC803 (Figure 6G, right). In addition, the reduced effect of miR-422a on MEF2D was verified in tissues of resected tumors from nude mice (Figure 6H). To understand whether miR-422a is directly targeting *MEF2D*, we cloned the *MEF2D* 3′ UTR fragment containing the miR-422a binding site downstream of the luciferase reporter gene (*MEF2D*-BS-WT) (Figure 6A). The mutated luciferase construct, in which mutations were introduced into the miR-422a binding site (*MEF2D*-BS-Mut), was also generated (Figure 6A). The luciferase assay showed that miR-422a induced a decrease in luciferase activity in pGL3-*MEF2D*-BS-WT-treated cells but not in pGL3-*MEF2D*-BS-Mut-treated cells (Figure 6I). Moreover, we found that overexpression of MEF2D reduced the effect of miR-422a on cell apoptosis (Figure 6J). These data suggest that miR-422a can directly bind to *MEF2D* mRNA and regulate its translation. In addition, our data indicate that MEF2D contributes to apoptosis resistance.

lncR-D63785 Promotes Development of Gastric Cancer by Targeting miR-442a and MEF2D

Our results demonstrated that lncR-D63785 has the ability to interact with miR-422a and that miR-422a directly binds to *MEF2D*, which led us to examine whether lncR-D63785 has a regulatory role in *MEF2D* expression. We analyzed the association of *MEF2D* and lncR-D63785 expression in GG tissues and found that there was a significant positive correlation between expression of these two molecules (Figure S8A). Knockdown of lncRNA-D6378 reduced the MEF2D level in BGC823 cells (Figure S8B) and in gastric cancer tissues from xenograft mice (Figure 7A), whereas overexpression of lncR-D63785 resulted in the upregulation of MEF2D (Figure S8C). Following exposure to DOX, the MEF2D expression level was significantly decreased in gastric cancer cells (Figure S8D) and xenograft tumors (Figures 7A and 7B). The combination of lncRNA-D6378 knockdown and DOX further reduced the MEF2D level in gastric cancer cells (Figure S8E) and *in vivo* (Figure 7A). Additionally, the level of MEF2D was also further reduced in miR-422a plus DOX-treated mice compared with mice treated with DOX alone (Figure 7B). These data indicate that lncR-D63785 has a regulatory role in tumor cell viability through the miR-422a and MEF2D pathway.

To better understand this signaling pathway, a luciferase reporter assay was used. The results showed that lncRNA-D6378 attenuated the inhibitory effect of miR-422a on the *MEF2D* binding site (Figure 7C). Next we examined whether the effect of lncRNA-D6378 on cell apoptosis is mediated via miR-422a and MEF2D in the presence of DOX. The results showed that knockdown of miR-422a attenuated DOX-induced cell apoptosis enhanced by silencing of lncR-D63785 (Figure 7D). Similarly, the inhibitory effect of lncR-D63785 on higher-dose DOX-induced cell apoptosis was reduced in *MEF2D* siRNA (Figure 7E). These results indicate that lncRNA-D6378 mediates gastric cancer cell resistance to apoptosis by modulating the miR-422a-MEF2D signaling pathway.

DISCUSSION

lncRNAs have important roles in various types of malignant tumors, including gastric cancer, which is one of the most commonly occurring malignancies in China.[1,17] Emerging evidence demonstrates that lncRNAs may function as novel diagnostic markers and indicators for treatment efficiency in gastric cancer.[18,19] The present work demonstrates that the expression level of lncR-D63785 is significantly increased in gastric cancer tumor tissue and cell lines. Despite the fact that only a small number of clinical gastric cancer samples were assessed in our study, a majority of tissue samples showed an elevation in the expression of lncR-D63785. Knockdown of lncR-D63785 inhibited cell proliferation, migration, and invasion and enhanced the sensitivity of gastric cancer cells to apoptosis induced by the anticancer drug DOX. Our findings reveal a novel mechanism regulating tumor suppression.

DOX is a DNA-intercalating agent that is widely used as a first-line clinical therapeutic regimen for a variety of cancers, including gastric cancer.[11–14] However, its application is limited by drug resistance and adverse effects because of a high dose level. To improve the efficiency of gastric cancer treatment, reversal of chemoresistance, an increase in the sensitivity of tumor cells to DOX, and a decrease in dose-dependent toxicities are all important.[12,14–16] Recently, several studies have documented that lncRNAs are involved in the resistance or sensitivity of tumors to chemotherapeutic drugs in gastric cancer. For example, PVT1 is highly expressed in gastric cancer tissues of DDP-resistant patients as well as in the BGC823 cells resistant to DDP and SGC7901 cells resistant to DDP.[49] Silencing of PVT1 in these cells could overcome resistance, whereas overexpression of PVT1 induced the apoptotic activity of cells.[49] Unlike PVT1, the level of LEIGC is lowered in cancer tissue and cell lines. Its overexpression can suppress tumor growth and cell proliferation, and it enhances the sensitivity of gastric cancer cells to 5-FU treatment by inhibiting epithelial-to-mesenchymal transition (EMT).[50] In our study, we found that lncR-D63785 expression could be influenced by DOX, and that silencing of lncR-D63785 not only reduces cell viability but also improves the sensitivity of gastric cancer cells to lower-dose DOX *in vitro* and *in vivo*. We also found that lncR-D63785 overexpression markedly decreased higher-dose DOX-induced cell apoptosis. These data indicate that lncR-D63785 is also associated with the development of drug resistance in gastric cancer and that downregulation of lncR-D63785 expression may be one of the mechanisms of DOX to induce tumor cell apoptosis. Currently, the underlying mechanisms leading to increased expression of lncR-D63785 in gastric cancer are unknown and still need to be explored in further detail. In addition, it would be interesting to observe the effects of lncR-D63785 in other tumor diseases.

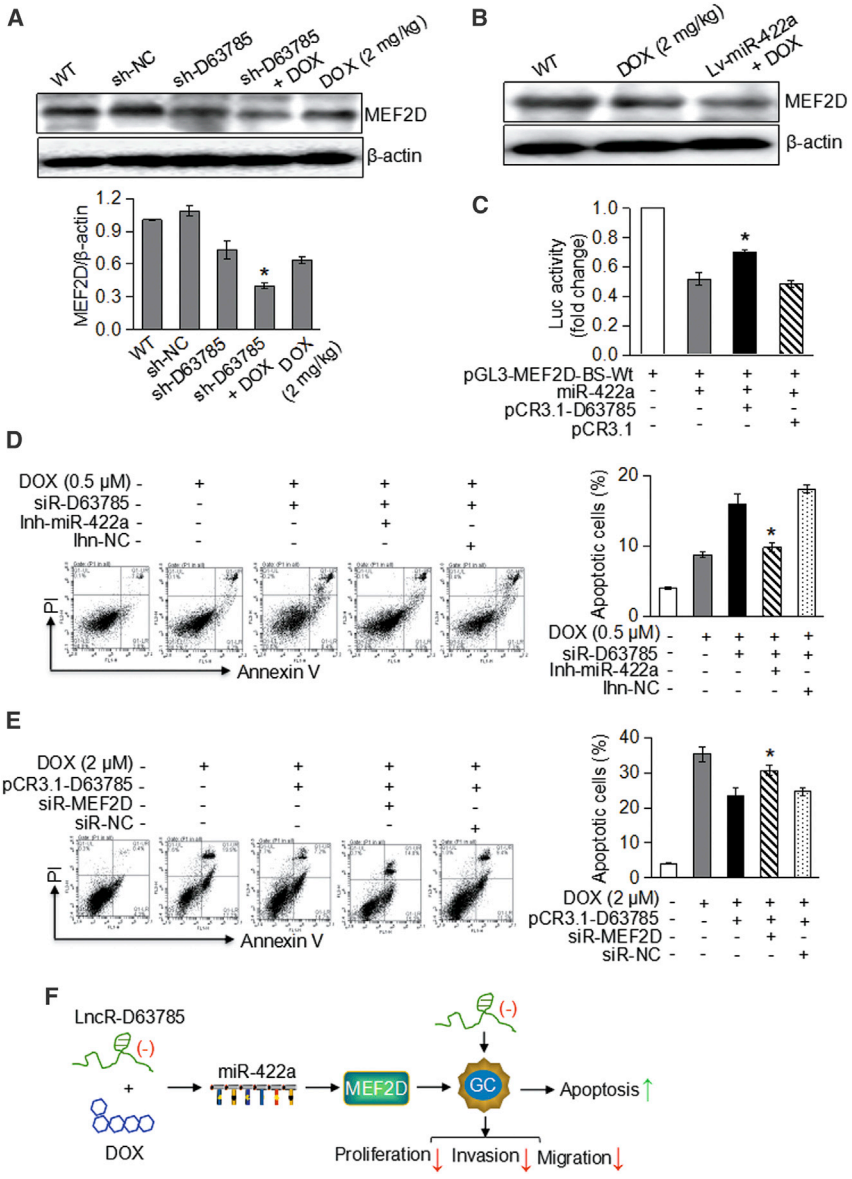

Figure 7. lncR-D63785 Regulates DOX-Induced Apoptosis by Targeting miR-422a and MEF2D

(A and B) The expression of MEF2D protein levels in tissues of xenograft tumors from the BALB/c nude mouse model was analyzed by western blotting, and the quantification of band intensity relative to β-actin intensity of (A) was quantified by MBF ImageJ software (down); *p < 0.05 versus the sh-NC group. (C) HEK293 cells were transfected with miR-422a or pCR3.1-D63785 or empty control, as indicated, and then with the luciferase constructs of pGL3-*MEF2D*-BS-WT. Luciferase activity was then analyzed to determine whether lncR-D63785 could counteract the inhibitory effect of miR-422a on MEF2D; *p < 0.05 versus pGL3-*MEF2D*-BS-WT and miR-422a. (D) BGC823 cells were infected with siR-D63785 and inh-miR-422a and exposed to 0.5 μM DOX. Then the apoptotic cells were analyzed by flow cytometry (left); the percentages of apoptotic cells are presented as a bar chart (right); *p < 0.05 versus DOX plus siR-D63785. (E) Apoptosis of BGC823 cells transfected with pCR3.1-D63785 and siR-*MEF2D* and exposed to 2 μM DOX was also detected by flow cytometry (left), and the percentages of apoptotic cells are presented as a bar chart (right); *p < 0.05 versus DOX plus pCR3.1-D63785. Data are expressed as the mean ± SD from at least three separate experiments. (F) A mechanism graph of the regulatory network and function of lncR-D63785. lncR-D63785 silencing could inhibit GC cell proliferation, migration, and invasion and enhance cell sensitivity to chemotherapeutic drugs through the miR-422a-MEF2D axis.

Several lncRNAs have been shown to act as miRNA sponges via base-pairing between them and sequestering the miRNAs from their target mRNAs, which, consequently, promotes mRNA translation. For example, MALAT-1 can upregulate Slug expression by inhibiting miR-1 expression in breast cancer.[33] In contrast, lncRNA-ATB upregulates ZEB1 and ZEB2 expression by competitively binding to the miR-200 family in hepatocellular carcinoma (HCC)[34] and gastric cancer.[35] H19 acts as a ceRNA for multiple targets, including let-7, miR-138, miR-200a, and miR-141, in different cancer types.[20,36,37] In this context, we found that lncR-D63785 could act as a ceRNA for miR-422a using the bioinformatics program RNAhybrid. Our experimental results *in vitro* and *in vivo* also confirmed this notion. Similar to our findings, another research group found that miR-422a is also regulated by the ceRNA network mediated by LINC00858, whose expression is dysregulated in NSCLC.[38] In our study, we found that LINC00858 was highly expressed in most gastric cancer cells (Figure S9), and further studies are warranted to deeply investigate the roles of LINC00858 in gastric cancer.

miR-422a has been shown to participate in the pathogenesis of a variety of cancers, including NSCLC,[38] glioblastoma,[39] osteosarcoma,[40] HCC,[41] head and neck squamous cell carcinoma,[42] and colorectal cancer.[43] Downregulation of miR-422a in these tumor tissues and cell lines contributes to the development of cancer. Experimental evidence indicates that overexpression of miR-422a suppresses the proliferation, migration, and invasion of tumor cells by directly targeting kallikerin-related peptidase 4 (*KLK4*),[38] *PIK3CA*,[39] forkhead box G1/Q1/E1 (*FOXG1/Q1/E1*),[41] or the *CD73* or *NT5E* oncogene.[42] In our study, we also observed a decrease in the level of miR-422a in gastric cancer tumor tissues and cell lines and that it has tumor suppression function by enhancing DOX-mediated tumor chemosensitivity. We also found that miR-422a could decrease the mRNA levels of *KLK4*, *FOXG1*, *FOXQ1*, and *FOXE1* but not *PIK3CA* or *CD73* (Figure S10). These results indicate that miR-422a is a target to promote DOX-induced

cell death, perhaps by targeting some mRNAs, such as *KLK4* and *FOXG1/Q1/E1*, which need to be studied further.

MEF2D is a member of the myocyte enhancer factor 2 (MEF2) family of transcription factors, consisting of 4 members in mammalian cells (MEF2A, MEF2B, MEF2C, and MEF2D), and it is upregulated in various types of tumors, including lung carcinoma,[44] osteosarcoma,[45] HCC,[46] leukemia,[47] and gastric cancer.[48] MEF2D expression is regulated by miRNAs, including miR-218,[44] miR-19,[47] miR-122,[51] and miR-421,[52] which play crucial roles in the development and progression of tumor cells. In our study, we found that MEF2D plays an important role in the oncogenic effects of lncR-D63785. These studies indicate that, besides miR-422a, the miRNAs mentioned above, except miR-19 (Figure S11), may also be correlated with lncR-D63785 in gastric cancer. Therefore, further studies are warranted to deeply investigate these additional relationships.

The oncogenic role of MEF2D has been well established in cancerous cells, and it accelerates cell proliferation, invasion, and metastasis via suppression of cell cycle arrest-associated genes, inhibition of apoptosis, promotion of the vascular endothelial growth factor (VEGF) signaling pathway and promoting the transforming growth factor β1 (TGF-β1) autoregulation circuitry, or other effects.[46,48,53] In lung cancer cells, MEF2D expression leads to resistance to CDDP treatment. A molecular study found that miR-1244 can control MEF2D expression; however, its expression is lowered in human lung cancer cells. Overexpression of miR-1244 significantly decreased the proliferation of CDDP-treated lung cancer by suppressing MEF2D.[54] On the contrary, MEF2D is downregulated in rhabdomyosarcoma (RMS) cells, in which it acts as a tumor suppressor by preventing the oncogenic growth properties of the aggressive alveolar rhabdomyosarcoma (ARMS) subtype of RMS.[55] In our study, we also found an oncogenic role of MEF2D in gastric cancer. Notably, we found that increased expression of MEF2D has an inhibitory effect on DOX-induced cell apoptosis. These results provide new insight into the role of MEF2D in tumor cell chemoresistance events.

In summary, we identified a new lncRNA, lncR-D63785, that acts as an oncogene in the development and progression of gastric cancer. Our results provide evidence for a link between lncR-D63785, miR-422a, and MEF2D in DOX-induced apoptosis and cell death resistance of gastric cancer cells (Figure 7F). Our study suggests that lncR-D63785 depletion alone or in combination with other chemotherapy could be a promising therapeutic strategy for gastric cancer. However, it remains to be investigated whether other miRNAs and/or molecules also participate in the ceRNA network involving lncR-D63785. It is also warranted that the expression pattern and function of lncRNA-D6378 in other types of tumors. Taken together, our data provide new evidence for the chemotherapeutic resistance of gastric cancer cells, and targeting the lncR-D63785-miR-422a-MEF2D axis may represent a promising therapeutic strategy for the diagnosis and treatment of gastric cancer.

MATERIALS AND METHODS

Tissue Samples

Human primary gastric cancer tissue samples and pair-matched adjacent non-tumorous tissues from 21 patients with gastric cancer were collected from Beijing Military General Hospital (Beijing, China). These gastric cancer patients were randomly selected from the clinical pool of the hospital's gastrointestinal clinic, and none of them received chemotherapy or radiotherapy. The collected tissues were immediately frozen in liquid nitrogen and stored at −80°C until use for analysis. Informed consent was obtained from all patients, and the study protocol was approved by the ethics committee of Beijing Military General Hospital.

Cell Lines

Human gastric cancer cells cell lines (GES-1, SGC7901, MGC803, BGC823, and NCI-N87) and HEK293 and HEK293T cells were cultured in RPMI 1640 medium (Gibco, Grand Island, NY, USA) or DMEM (Gibco, Grand Island, NY, USA) containing 10% fetal bovine serum, 100 units/mL penicillin, and 100 g/mL streptomycin. These cell lines were used within 2 weeks of recovery, and they were incubated at 37°C with 5% CO_2 in a humidified atmosphere.

Real-Time qPCR

Total RNA of tissue samples or cells were extracted with TRIzol reagent (Invitrogen, Carlsbad, CA, USA) according to the manufacturer's instructions. cDNA was generated with random primers and Moloney murine leukemia virus reverse transcriptase (Takara, Otsu, Japan) according to the manufacturer's protocol. The expression of genes or miRNA was detected using the real-time qPCR method, which was performed using SYBR Green Supermix (Roche, IN, USA) on an iCycler iQ real-time PCR system (Bio-Rad). The primers used for lncR-D63785, LINC00858, miR-422a, miR-19, *MEF2D*, *KLK4*, *FOXG1*, *FOXQ1*, *FOXE1*, *PIK3CA*, *CD73*, *GAPDH*, and U6 are shown in Table S1. Data were normalized to *GAPDH* or U6 expression. In addition, real-time qPCR for miR-422a in gastric cancer cell lines was also performed using miScript primer assays and the SYBR Green PCR Kit according to the manufacturer's instructions (QIAGEN, Hilden, Germany).

RNAi

Three siRNAs (siR-#1, siR-#2, and siR-#3) targeting different regions of lncR-D63785 were synthesized by Ribobio (Guangzhou, China). Among them, siR-#2 (named siR-D63785) produced the best inhibitory effect on lncR-D63785 expression, and the sequence of siR-D63785 was 5′-GGCAGATTCCACAGAATTT-3′. The sequence of siR-*MEF2D* was 5′-UAUGAGCUGAGCGUGCUTT-3′. The sequence of the control siRNA (named siR-NC) was 5′-CAG TACTTTTGTGTAGTACAA-3′. The siRNAs were transfected into BGC823 cells using Lipofectamine 2000 (Invitrogen) according to the manufacturer's protocol.

Plasmid Construction

To construct pCR3.1-D63785, which constitutively expresses human lncR-D63785 under the human cytomegalovirus (CMV)

immediate-early promoter, the sequence of lncR-D63785 was amplified by PCR with primers F (5′-CGGAATTCTTGCTGCTGACACGCCGA-3′) and R (5′-ACGCGTCGACACTGACGTATTTCTGGACCCACT-3′). The PCR products were ligated to the T-A cloning vector pBS-T (Tiangen, Beijing, China), and the recombinant plasmid was digested with EcoRI and SalI to retrieve the lncR-D63785 fragment, which was inserted into pCR3.1 (Invitrogen, Carlsbad, CA, USA) at the EcoRI and SalI sites. The eukaryotic expression vector of the *MEF2D* gene (named pKC-*EF1a-IRES-eGFP-neoR-MEF2D*; pKC-*EF1a-MEF2D* for short) and its control plasmid pKC-*EF1a-RED2* were gifts from Affiliated Hospital of Qingdao University and used for overexpression assays.

MTT Assay

Gastric cancer cells were cultured in a 96-well culture plate at a density of 1×10^4 cells/cm^2, and then they were transfected with siR-D63785 or siR-NC for the indicated times (20 hr, 44 hr, 68 hr, and 92 hr). After the incubation time, 20 μL of 5 mg/mL MTT (Sangon, Shanghai, China) was added to each well and incubated for another 4 hr. The formed reduced formazan was dissolved by addition of 200 μL DMSO, and the culture plate was shaken for 10 min at room temperature. Each well was assessed by microreader (SpectraMax i3, Molecular Devices, USA) at 490 nm.

EdU Incorporation Assay

Gastric cancer cells were seeded into 96-well cell culture plates at a density of 1×10^4 cells/well. When the cells were treated with lncR-D63785 knockdown or mR-422a, 10 μmol/L EdU (Roche Diagnostics, Mannheim, Germany) was added 24 hr prior to the end of the test reagent incubation and allowed to incorporate into proliferating cells. After fixation with ice-cold 4% paraformaldehyde for 30 min at room temperature, the cells were washed three times with PBS and neutralized with glycine (2 mg/mL) for 10 min. After washing, the cells were incubated in PBS containing 0.1% Triton X-100 (PBST) for 30 min. Next, the cells were washed three times with PBS and labeled with 5 μg/mL of Hoechst 33342 for 1 hr at 37°C. EdU-positive proliferating cells are expressed as a percentage of the control level.

Transwell Assay

To determine the ability of gastric cancer cells to migrate, cells (1×10^4/mL) in serum-free medium were added to an inner cup of a 48-well transwell chamber (Corning Life Sciences, Corning, New York) containing 200 μL of serum-free RPMI 1640 medium. Medium containing 10% fetal bovine serum (FBS) was then added to the lower chamber as a chemoattractant. After incubation for 48 hr at 37°C in a humidified atmosphere containing 5% CO_2, the non-migrating cells on the polycarbonate membranes were removed with a cotton swab. The polycarbonate membranes were then incubated with 4% paraformaldehyde for 30 min and stained with 0.2% crystal violet for 20 min. The number of cells that had crossed through the polycarbonate membranes was recorded and analyzed. For the cell invasion assay, Matrigel (Corning Life Sciences, Corning, New York) was thawed overnight at 4°C and diluted with serum-free RPMI 1640 medium (1:10). The membrane at the bottom of the transwell chamber was coated with 50 μL Matrigel suspension, followed by incubation for 1 hr at room temperature. Similarly, cells (1×10^4 cells/mL) were allowed to migrate for 48 hr toward the lower chamber filled with 10% FBS as a chemoattractant. The upper layer of cells on the membrane was then removed, and the cells that had invaded through the membrane were fixed, stained, and counted. Three randomly selected fields were assessed for the number of invaded cells as follows: number of invaded cells = (number of cells in all three fields)/3.

Apoptosis Assay

Gastric cancer cells were distributed in 6-well tissue culture plates (1×10^5 cells/well) in DMEM containing 10% FBS. The cells were then transfected with siRNA and exposed or not to DOX for 24 hr. The cells were then harvested and stained with fluorescein isothiocyanate (FITC)-conjugated Annexin V and the propidium iodide (PI) cell apoptosis detection kit (Majorbio Biotech, Shanghai, China) following the manufacturer's instructions. The results were measured using a FACSCalibur system (BD Biosciences, USA) and analyzed with Flow Jo 7.6.1.

Lentivirus Production and Transduction

For virus creation, HEK293T cells were passaged to maintain them at 30%–40% confluence on the following day. Cells were transfected using Lipofectamine 2000 (Invitrogen, Carlsbad, CA, USA) according to the manufacturer's instructions. The shRNAs targeting lncR-D63785 (sense, 5′-ATCAGGCCGGCAGGTCTGTGCTGACCCCAGTGAGGAGTGGGTCCAGAAATACGTCAGTA-3′; antisense, 5′-CTAGTACTGACGTATTTCTGGACCCACTCCTCACTGGGGTCAGCACAGACCTGCCGGCCTGAT-3′) or miR-422a (sense, 5′-CCGGACTGGACTTAGGGTCAGAAGGCCTCGAGGCCTTCTGACCCTAAGTCCAGTTTTTTG-3′); antisense, 5′-AATTCAAAAAACTGGACTTAGGGTCAGAAGGCCTCGAGGCCTTCTGACCCTAAGTCCAGT-3′) were annealed and cloned into the pLKO.1-shRNA-EGFP vector (Addgene, Cambridge, MA). The vectors were then transfected with the packaging vectors (psPAX2 and pMD2.G) into HEK293T cells using Lipofectamine 2000 (Invitrogen) to produce the lentivirus. The transfection mixture was added to its respective plates and incubated overnight. After 24 hr, the transfection medium was removed and replaced with fresh medium. After an additional 48 hr and 72 hr, cell medium containing shRNA lentivirus was collected and filtered for use. For target cell transduction, BGC823 cells were passaged to 40% confluence on the following day. The viral medium was added to cells with 8 μg/mL polybrene four times over 2 days. After 7 days of transduction, the viral medium was removed, and the cells were collected for further experiments.

Human Tumor-Bearing Nude Mice

Male athymic nude mice (Balb-nu/nu, 5 weeks old) were purchased from the Beijing Experimental Animal Center (Chinese Academy of Sciences, Beijing, China) and maintained at an animal facility under pathogen-free conditions. The handling of mice and experimental procedures were conducted in accordance with experimental animal guidelines and were approved by the Committee on the Ethics of Animal Experiments of Qingdao University. The mice were randomly

assigned to groups, with six mice in each group. BGC823 cells (1.5×10^6 or 2×10^6) transfected with sh-D63785, Lv-miR-422a, or Lv-NC were harvested and resuspended in PBS (100 μL), and then they were subcutaneously injected into the right flanks of the mice. Beginning on the ninth or 15th day, when the tumors had reached a size of 250–300 mm^3, the mice received the indicated treatment. Mice received DOX (2 mg/kg) by intraperitoneal injection every other day, whereas control mice received a corresponding volume of PBS. The treated mice were sacrificed on day 30 or 35, and the tumor volume was calculated as length × $width^2/2$.

Cell Transfection with miRNA Duplexes or Inhibitors

The miR-422a duplexes were synthesized by GenePharma. The miR-422a mimic sequence was 5′-ACUGGACUUAGGGUCAGAAG GC-3′. The mimic control sequence was 5′-UUCUCCGAACGUGU CACGUTT-3′. A chemically modified antisense oligonucleotide (inhibitor) was used to inhibit endogenous miR-422a -expression. The inhibitor sequence was 5′-GCCUUCUGACCCUAAGUC CAGU-3′. The inhibitor control sequence was 5′-UUCUCCGAAC GUGUCACGUTT-3′. All bases were 2′-O-methyl-modified (GenePharma). The cells were transfected with miRNA duplexes (100 nM) or inhibitors (200 nM) using Lipofectamine 2000 (Invitrogen) according to the manufacturer's instructions.

Reporter Constructs and Luciferase Assay

The fragment of lncR-D63785 cDNA containing the miR-422a binding site (D63785-BS-WT) was synthesized. The synthesized oligonucleotides were as follows: sense, 5′-ATCAGGCCGGCAGGTCTG TGCTGACCCCAGTGAGGAGTGGGTCCAGAAATACGTCAG TA-3′; antisense, 5′-CTAGTACTGACGTATTTCTGGACCCACTC CTCACTGGGGTCAGCACAGACCTGCCGGCCTGAT-3′. The sense and antisense oligonucleotides were annealed, and the annealed oligonucleotides were cloned into the pGL3 vector (Promega, Madison, WI, USA) immediately downstream of the stop codon of the luciferase gene. The mutant of lncR-D63785 BS (D63785-BS-Mut) was cloned in the same manner. The synthesized oligonucleotides for D63785-BS-Mut were as follows: sense, 5′-ATCAGGCCGGCA CAAGCGTGCTGACCCCAGTGAGGAGTGGCCAACCAAATAC GTCAGTA-3′; anti-sense, 5′-CTAGTACTGACGTATTTGGTTG GCCACTCCTCACTGGGGTCAGCACGCTTCTGCCGGCCTG AT-3′. The fragment of *MEF2D* cDNA containing the miR-422a binding site (*MEF2D*-BS-WT) was synthesized with binding sequence 335. The synthesized oligonucleotides were as follows: sense, 5′-CGGGGTACCCCTTGGGGTCTCCCAGTCTA-3′; antisense, 5′-CCGCTCGAGACTTGATGCTGATGTGGGGG-3′. The mutant of *MEF2D* (*MEF2D*-BS-Mut) with binding sequence 335 was constructed by BGI Sequencing (China). The annealed oligonucleotides were then cloned into the pGL3 vector (Promega, Madison) as described above. For the luciferase assay, HEK293 cells in 24-well plates were co-transfected with 200 ng/well luciferase reporter constructs, 400 ng/well miR-422a mimic, or mimic control using Lipofectamine 2000 (Invitrogen). As an internal control, 5 ng/well simian virus (SV)-*Renilla* luciferase plasmid was used. The cells were harvested 24 h after transfection, and the luciferase activity was detected using the Dual Luciferase Reporter Assay Kit (Promega) according to the manufacturer's instructions. Thirty microliters of the protein samples were analyzed using a luminometer. The activity of firefly luciferase was normalized to that of *Renilla* luciferase.

Pull-Down Assay with Biotinylated miRNA

The pull-down assay was performed as we described previously.[56] Briefly, miR-422a and miR-422a-Mut single-stranded RNAs were synthesized and labeled with biotin at 5′. The miR-422a-WT sequence was 5′-ACUGGACUUAGGTCAGAAGGC-3′, the miR-422a-Mut sequence was 5′-AGGCCACUUAGGUCACGGAAC-3′, and the miR-NC sequence was 5′-UUCUCCGAACGUGUCAC GUUU-3′. BGC823 cells were transfected with biotinylated miRNAs and harvested 24 hr after transfection. The cells were washed with PBS, followed by brief vortexing and incubation in lysis buffer (20 mM Tris-HCl [pH 7.5], 200 mM NaCl, 2.5 mM $MgCl_2$, 60 U/mL RNase inhibitor, 1 mM DTT, and protease inhibitor) on ice for 30 min. The lysate was precleared by centrifugation and incubated with streptavidin agarose beads (Invitrogen). To prevent non-specific binding of RNA and protein complexes, the beads were coated with 1% RNase-free BSA (Sigma) and 0.5 mg/mL yeast tRNA (Sigma). The beads were incubated at 4°C for 3 hr and then washed twice with ice-cold lysis buffer, three times with low-salt buffer (0.1% SDS, 1% Triton X-100, 2 mM EDTA, 20 mM Tris-HCl [pH 8.0], and 150 mM NaCl), and once with high-salt buffer (0.1% SDS, 1% Triton X-100, 2 mM EDTA, 20 mM Tris-HCl [pH 8.0], and 500 mM NaCl). The bound RNAs were purified for analysis using TRIzol. The levels of lncR-D63785 in the RNA samples were detected by real-time qPCR.

Western Blotting

The cells were lysed for 30 min on ice in radioimmunoprecipitation assay (RIPA) lysis buffer (Solarbio, Beijing, China) containing 0.1 mM PMSF and a cocktail of protease inhibitors (Roche). The samples were subjected to 12% SDS-PAGE and transferred to nitrocellulose membranes. Then the blots were probed using primary antibodies, including anti-MEF2D monoclonal antibody (mAb) (BD Biosciences, San Jose, CA, USA) and anti-GAPDH mAb (Santa Cruz Biotechnology, CA, USA) or anti-β-actin mAb (Santa Cruz). After four washes with PBS-Tween 20, horseradish peroxidase-conjugated secondary antibodies were added. The signals were detected with an enhanced chemiluminescence (ECL) system (Pierce, Rockford, IL, USA) according to the directions of the manufacturer and then exposed on X-ray film (Kodak, Rochester, NY, USA).

Statistical Analysis

All statistical analyses were performed using the SPSS 13.0 statistical software package. The results are expressed as means ± SD of at least three independent experiments. The differences among experimental groups were evaluated by one-way ANOVA. Paired data were determined by two-tailed Student's t test. $p < 0.05$ was considered statistically significant.

SUPPLEMENTAL INFORMATION

Supplemental Information includes eleven figures and one table and can be found with this article online at https://doi.org/10.1016/j.omtn.2018.05.024.

AUTHOR CONTRIBUTIONS

Conception and Design, J.W., P.L., and Y.W.; Development and Methodology, J.W., P.L., and Z.L.; Acquisition of Data, Z.Z., Z.L., Y.H., and X.P.; Analysis and Interpretation of Data: Z.Z., Z.L., Y.H., X.P., and P.S.; Writing, Review, and/or Revision of the Manuscript, Z.Z., J.W., M.P., and M.A.T.; Administrative, Technical, and Material Support, Y.H., Y.W., and X.A.; Study Supervision, J.W.

CONFLICTS OF INTEREST

The authors declare no conflicts of interest.

ACKNOWLEDGMENTS

We thank Jia Liu for the gifts of pKC-*EF1α-RED2* and pKC-*EF1α-MEF2D*. This study was supported by the National Natural Science Foundation of China (81502063, 31430041, 31671447, and 81741173), Basic Research Project of Qingdao Source Innovation Program (18-2-2-76-jch), A Project of Shandong Province Higher Educational Science and Technology Program (J18KA290) and the Key Science and Technology Program of Shandong Province (jk47).

REFERENCES

1. Aoyama, T., and Yoshikawa, T. (2017). Adjuvant therapy for locally advanced gastric cancer. Surg. Today *47*, 1295–1302.
2. Smyth, E.C., and Cunningham, D. (2013). Gastric cancer in 2012: Defining treatment standards and novel insights into disease biology. Nat. Rev. Clin. Oncol. *10*, 73–74.
3. Cheetham, S.W., Gruhl, F., Mattick, J.S., and Dinger, M.E. (2013). Long noncoding RNAs and the genetics of cancer. Br. J. Cancer *108*, 2419–2425.
4. Maruyama, R., Suzuki, H., Yamamoto, E., Imai, K., and Shinomura, Y. (2012). Emerging links between epigenetic alterations and dysregulation of noncoding RNAs in cancer. Tumour Biol. *33*, 277–285.
5. Fang, X.Y., Pan, H.F., Leng, R.X., and Ye, D.Q. (2015). Long noncoding RNAs: novel insights into gastric cancer. Cancer Lett. *356* (2 Pt B), 357–366.
6. Correa, P. (2013). Gastric cancer: overview. Gastroenterol. Clin. North Am. *42*, 211–217.
7. Wilhelm, F., Simon, E., Böger, C., Behrens, H.M., Krüger, S., and Röcken, C. (2017). Novel insights into gastric cancer: Methylation of r-spondins and regulation of lgr5 by sp1. Mol. Cancer Res. *15*, 776–785.
8. Piazuelo, M.B., and Correa, P. (2013). Gastric cáncer: Overview. Colomb. Med. *44*, 192–201.
9. Mirski, S.E., Gerlach, J.H., and Cole, S.P. (1987). Multidrug resistance in a human small cell lung cancer cell line selected in adriamycin. Cancer Res. *47*, 2594–2598.
10. Pathan, R.A., Singh, B.K., Pillai, K.K., and Dubey, K. (2010). Naproxen aggravates doxorubicin-induced cardiomyopathy in rats. Indian J. Pharmacol. *42*, 44–49.
11. Zhang, X., Peng, X., Yu, W., Hou, S., Zhao, Y., Zhang, Z., Huang, X., and Wu, K. (2011). Alpha-tocopheryl succinate enhances doxorubicin-induced apoptosis in human gastric cancer cells via promotion of doxorubicin influx and suppression of doxorubicin efflux. Cancer Lett. *307*, 174–181.
12. Bamodu, O.A., Huang, W.C., Tzeng, D.T., Wu, A., Wang, L.S., Yeh, C.T., and Chao, T.Y. (2015). Ovatodiolide sensitizes aggressive breast cancer cells to doxorubicin, eliminates their cancer stem cell-like phenotype, and reduces doxorubicin-associated toxicity. Cancer Lett. *364*, 125–134.
13. Zou, P., Chen, M., Ji, J., Chen, W., Chen, X., Ying, S., Zhang, J., Zhang, Z., Liu, Z., Yang, S., and Liang, G. (2015). Auranofin induces apoptosis by ROS-mediated ER stress and mitochondrial dysfunction and displayed synergistic lethality with piperlongumine in gastric cancer. Oncotarget *6*, 36505–36521.
14. Neuzil, J., Dong, L.F., Ramanathapuram, L., Hahn, T., Chladova, M., Wang, X.F., Zobalova, R., Prochazka, L., Gold, M., Freeman, R., et al. (2007). Vitamin E analogues as a novel group of mitocans: anti-cancer agents that act by targeting mitochondria. Mol. Aspects Med. *28*, 607–645.
15. Wang, J., Feng, C., He, Y., Ding, W., Sheng, J., Arshad, M., Zhang, X., and Li, P. (2015). Phosphorylation of apoptosis repressor with caspase recruitment domain by protein kinase CK2 contributes to chemotherapy resistance by inhibiting doxorubicin induced apoptosis. Oncotarget *6*, 27700–27713.
16. Wu, H., Liu, S., Gong, J., Liu, J., Zhang, Q., Leng, X., Zhang, N., and Li, Y. (2017). VCPA, a novel synthetic derivative of α-tocopheryl succinate, sensitizes human gastric cancer to doxorubicin-induced apoptosis via ROS-dependent mitochondrial dysfunction. Cancer Lett. *393*, 22–32.
17. Chen, J., Wang, R., Zhang, K., and Chen, L.B. (2014). Long non-coding RNAs in non-small cell lung cancer as biomarkers and therapeutic targets. J. Cell. Mol. Med. *18*, 2425–2436.
18. Clark, M.B., and Mattick, J.S. (2011). Long noncoding RNAs in cell biology. Semin. Cell Dev. Biol. *22*, 366–376.
19. Deniz, E., and Erman, B. (2017). Long noncoding RNA (lincRNA), a new paradigm in gene expression control. Funct. Integr. Genomics *17*, 135–143.
20. Zhou, X., Ye, F., Yin, C., Zhuang, Y., Yue, G., and Zhang, G. (2015). The interaction between mir-141 and lncrna-h19 in regulating cell proliferation and migration in gastric cancer. Cell. Physiol. Biochem. *36*, 1440–1452.
21. Chen, F.J., Sun, M., Li, S.Q., Wu, Q.Q., Ji, L., Liu, Z.L., Zhou, G.Z., Cao, G., Jin, L., Xie, H.W., et al. (2013). Upregulation of the long non-coding RNA HOTAIR promotes esophageal squamous cell carcinoma metastasis and poor prognosis. Mol. Carcinog. *52*, 908–915.
22. Wang, S.S., Wuputra, K., Liu, C.J., Lin, Y.C., Chen, Y.T., Chai, C.Y., Lin, C.S., Kuo, K.K., Tsai, M.H., Wang, S.W., et al. (2016). Oncogenic function of the homeobox A13-long noncoding RNA HOTTIP-insulin growth factor-binding protein 3 axis in human gastric cancer. Oncotarget *7*, 36049–36064.
23. Huang, M., Hou, J., Wang, Y., Xie, M., Wei, C., Nie, F., Wang, Z., and Sun, M. (2017). Long Noncoding RNA LINC00673 Is Activated by SP1 and Exerts Oncogenic Properties by Interacting with LSD1 and EZH2 in Gastric Cancer. Mol. Ther. *25*, 1014–1026.
24. Zhang, N., Wang, A.Y., Wang, X.K., Sun, X.M., and Xue, H.Z. (2016). GAS5 is downregulated in gastric cancer cells by promoter hypermethylation and regulates adriamycin sensitivity. Eur. Rev. Med. Pharmacol. Sci. *20*, 3199–3205.
25. Sun, M., Jin, F.Y., Xia, R., Kong, R., Li, J.H., Xu, T.P., Liu, Y.W., Zhang, E.B., Liu, X.H., and De, W. (2014). Decreased expression of long noncoding RNA GAS5 indicates a poor prognosis and promotes cell proliferation in gastric cancer. BMC Cancer *14*, 319.
26. Zhao, J., Dahle, D., Zhou, Y., Zhang, X., and Klibanski, A. (2005). Hypermethylation of the promoter region is associated with the loss of MEG3 gene expression in human pituitary tumors. J. Clin. Endocrinol. Metab. *90*, 2179–2186.
27. Sun, M., Xia, R., Jin, F., Xu, T., Liu, Z., De, W., and Liu, X. (2014). Downregulated long noncoding RNA MEG3 is associated with poor prognosis and promotes cell proliferation in gastric cancer. Tumour Biol. *35*, 1065–1073.
28. Wang, Y., Zhang, D., Wu, K., Zhao, Q., Nie, Y., and Fan, D. (2014). Long noncoding RNA MRUL promotes ABCB1 expression in multidrug-resistant gastric cancer cell sublines. Mol. Cell. Biol. *34*, 3182–3193.
29. Zhang, Y., Song, X., Wang, X., Hu, J., and Jiang, L. (2016). Silencing of lncrna hulc enhances chemotherapy induced apoptosis in human gastric cancer. J. Med. Biochem. *35*, 137–143.
30. Shang, C., Guo, Y., Zhang, J., and Huang, B. (2016). Silence of long noncoding RNA UCA1 inhibits malignant proliferation and chemotherapy resistance to adriamycin in gastric cancer. Cancer Chemother. Pharmacol. *77*, 1061–1067.
31. Ebert, M.S., Neilson, J.R., and Sharp, P.A. (2007). MicroRNA sponges: competitive inhibitors of small RNAs in mammalian cells. Nat. Methods *4*, 721–726.

32. Li, L.J., Zhao, W., Tao, S.S., Leng, R.X., Fan, Y.G., Pan, H.F., and Ye, D.Q. (2017). Competitive endogenous RNA network: potential implication for systemic lupus erythematosus. Expert Opin. Ther. Targets *21*, 639–648.

33. Jin, C., Yan, B., Lu, Q., Lin, Y., and Ma, L. (2016). Reciprocal regulation of Hsa-miR-1 and long noncoding RNA MALAT1 promotes triple-negative breast cancer development. Tumour Biol. *37*, 7383–7394.

34. Yuan, J.H., Yang, F., Wang, F., Ma, J.Z., Guo, Y.J., Tao, Q.F., Liu, F., Pan, W., Wang, T.T., Zhou, C.C., et al. (2014). A long noncoding RNA activated by TGF-β promotes the invasion-metastasis cascade in hepatocellular carcinoma. Cancer Cell *25*, 666–681.

35. Saito, T., Kurashige, J., Nambara, S., Komatsu, H., Hirata, H., Ueda, M., Sakimura, S., Uchi, R., Takano, Y., Shinden, Y., et al. (2015). A long non-coding RNA activated by transforming growth factor-β is an independent prognostic marker of gastric cancer. Ann. Surg. Oncol. *22* (*Suppl 3*), S915–S922.

36. Ma, C., Nong, K., Zhu, H., Wang, W., Huang, X., Yuan, Z., and Ai, K. (2014). H19 promotes pancreatic cancer metastasis by derepressing let-7's suppression on its target HMGA2-mediated EMT. Tumour Biol. *35*, 9163–9169.

37. Liang, W.C., Fu, W.M., Wong, C.W., Wang, Y., Wang, W.M., Hu, G.X., Zhang, L., Xiao, L.J., Wan, D.C., Zhang, J.F., and Waye, M.M. (2015). The lncRNA H19 promotes epithelial to mesenchymal transition by functioning as miRNA sponges in colorectal cancer. Oncotarget *6*, 22513–22525.

38. Zhu, S.P., Wang, J.Y., Wang, X.G., and Zhao, J.P. (2017). Long intergenic non-protein coding RNA 00858 functions as a competing endogenous RNA for miR-422a to facilitate the cell growth in non-small cell lung cancer. Aging (Albany N.Y.) *9*, 475–486.

39. Liang, H., Wang, R., Jin, Y., Li, J., and Zhang, S. (2016). MiR-422a acts as a tumor suppressor in glioblastoma by targeting PIK3CA. Am. J. Cancer Res. *6*, 1695–1707.

40. Liu, M., Xiusheng, H., Xiao, X., and Wang, Y. (2016). Overexpression of miR-422a inhibits cell proliferation and invasion, and enhances chemosensitivity in osteosarcoma cells. Oncol. Rep. *36*, 3371–3378.

41. Zhang, J., Yang, Y., Yang, T., Yuan, S., Wang, R., Pan, Z., Yang, Y., Huang, G., Gu, F., Jiang, B., et al. (2015). Double-negative feedback loop between microRNA-422a and forkhead box (FOX)G1/Q1/E1 regulates hepatocellular carcinoma tumor growth and metastasis. Hepatology *61*, 561–573.

42. Bonnin, N., Armandy, E., Carras, J., Ferrandon, S., Battiston-Montagne, P., Aubry, M., Guihard, S., Meyronet, D., Foy, J.P., Saintigny, P., et al. (2016). MiR-422a promotes loco-regional recurrence by targeting NT5E/CD73 in head and neck squamous cell carcinoma. Oncotarget *7*, 44023–44038.

43. Zheng, G.X., Qu, A.L., Yang, Y.M., Zhang, X., Zhang, S.C., and Wang, C.X. (2016). miR-422a is an independent prognostic factor and functions as a potential tumor suppressor in colorectal cancer. World J. Gastroenterol. *22*, 5589–5597.

44. Song, L., Li, D., Zhao, Y., Gu, Y., Zhao, D., Li, X., Bai, X., Sun, Y., Zhang, X., Sun, H., et al. (2016). miR-218 suppressed the growth of lung carcinoma by reducing MEF2D expression. Tumour Biol. *37*, 2891–2900.

45. Yu, H., Sun, H., Bai, Y., Han, J., Liu, G., Liu, Y., and Zhang, N. (2015). MEF2D overexpression contributes to the progression of osteosarcoma. Gene *563*, 130–135.

46. Ma, L., Liu, J., Liu, L., Duan, G., Wang, Q., Xu, Y., Xia, F., Shan, J., Shen, J., Yang, Z., et al. (2014). Overexpression of the transcription factor MEF2D in hepatocellular carcinoma sustains malignant character by suppressing G2-M transition genes. Cancer Res. *74*, 1452–1462.

47. Canté-Barrett, K., Pieters, R., and Meijerink, J.P.P. (2014). Myocyte enhancer factor 2C in hematopoiesis and leukemia. Oncogene *33*, 403–410.

48. Xu, K., and Zhao, Y.C. (2016). MEF2D/Wnt/β-catenin pathway regulates the proliferation of gastric cancer cells and is regulated by microRNA-19. Tumour Biol. *37*, 9059–9069.

49. Zhang, X.W., Bu, P., Liu, L., Zhang, X.Z., and Li, J. (2015). Overexpression of long non-coding RNA PVT1 in gastric cancer cells promotes the development of multidrug resistance. Biochem. Biophys. Res. Commun. *462*, 227–232.

50. Han, Y., Ye, J., Wu, D., Wu, P., Chen, Z., Chen, J., Gao, S., and Huang, J. (2014). LEIGC long non-coding RNA acts as a tumor suppressor in gastric carcinoma by inhibiting the epithelial-to-mesenchymal transition. BMC Cancer *14*, 932.

51. Qiu, Y., Yang, J., Bian, S., Chen, G., and Yu, J. (2016). PPARγ suppresses the proliferation of cardiac myxoma cells through downregulation of MEF2D in a miR-122-dependent manner. Biochem. Biophys. Res. Commun. *474*, 560–565.

52. Liu, L., Cui, S., Zhang, R., Shi, Y., and Luo, L. (2017). MiR-421 inhibits the malignant phenotype in glioma by directly targeting MEF2D. Am. J. Cancer Res. *7*, 857–868.

53. Yu, W., Huang, C., Wang, Q., Huang, T., Ding, Y., Ma, C., Ma, H., and Chen, W. (2014). MEF2 transcription factors promotes EMT and invasiveness of hepatocellular carcinoma through TGF-β1 autoregulation circuitry. Tumour Biol. *35*, 10943–10951.

54. Li, G.J., Zhao, G.Q., Yang, J.P., Zhou, Y.C., Yang, K.Y., Lei, Y.J., and Huang, Y.C. (2017). Effect of miR-1244 on cisplatin-treated non-small cell lung cancer via MEF2D expression. Oncol. Rep. *37*, 3475–3483.

55. Zhang, M., Truscott, J., and Davie, J. (2013). Loss of MEF2D expression inhibits differentiation and contributes to oncogenesis in rhabdomyosarcoma cells. Mol. Cancer *12*, 150.

56. Wang, J.X., Zhang, X.J., Li, Q., Wang, K., Wang, Y., Jiao, J.Q., Feng, C., Teng, S., Zhou, L.Y., Gong, Y., et al. (2015). Microrna-103/107 regulate programmed necrosis and myocardial ischemia/reperfusion injury through targeting fadd. Circ. Res. *117*, 352–363.